



Celorrio, V., Quaino, P., Santos, E., Florez-Montano, J., Humphrey, J., Guillen-Villafuerte, O., Plana, D., Lazaro, M. J., Pastor, E., & Fermin, D. (2017). Strain Effects on the Oxidation of CO and HCOOH at Au-Pd Core-Shell Nanoparticles. *ACS Catalysis*, 7(3), 1673-1680.
<https://doi.org/10.1021/acscatal.6b03237>

Publisher's PDF, also known as Version of record

License (if available):
CC BY

Link to published version (if available):
[10.1021/acscatal.6b03237](https://doi.org/10.1021/acscatal.6b03237)

[Link to publication record in Explore Bristol Research](#)
PDF-document

This is the final published version of the article (version of record). It first appeared online via ACS at <http://pubs.acs.org/doi/abs/10.1021/acscatal.6b03237>. Please refer to any applicable terms of use of the publisher.

University of Bristol - Explore Bristol Research

General rights

This document is made available in accordance with publisher policies. Please cite only the published version using the reference above. Full terms of use are available:
<http://www.bristol.ac.uk/red/research-policy/pure/user-guides/ebr-terms/>

Supporting Information

Strain Effects on the Oxidation of CO and HCOOH at Au-Pd Core-Shell Nanoparticles

Verónica Celorrio,[†] Paola M. Quaino,[‡] Elizabeth Santos,^{§,ϕ} Jonathan Flórez-Montaño,[‡]

Jo J.L. Humphrey,[†] Olmedo Guillén-Villafuerte,[‡] Daniela Plana,[†] María J. Lázaro,[§]

Elena Pastor,^{‡} and David J. Fermín^{†*}*

[†] School of Chemistry, University of Bristol, Cantocks Close, Bristol BS8 1TS, UK

[‡] Instituto de Química Aplicada del Litoral, IQAL (UNL-CONICET), PRELINE (FIQ-UNL), Santa Fe, Argentina.

[§] Instituto de Física Enrique Gaviola (IFEG-CONICET), Facultad de Matemática, Astronomía y Física, FaMAF-UNC. Cordoba, Argentina.

^ϕ Institute of Theoretical Chemistry, Ulm University. Albert-Einstein-Allee 11, Ulm, Germany.

[‡] Departamento de Química e Instituto de Materiales y Nanotecnología, Universidad de La Laguna, Avda. Astrofísico Francisco Sánchez s/n, 38206 La Laguna, Tenerife, Spain

[§] Instituto de Carboquímica (CSIC), Miguel Luesma Castán 4, 50018 Zaragoza, Spain

AUTHOR INFORMATION

Corresponding Authors

*E-mail: E.Pastor@ull.es (E.P.)

*E-mail: David.Fermin@bristol.ac.uk (D.J.F)

S1. FURTHER EXPERIMENTAL AND COMPUTATIONAL INFORMATION

Preparation of the electrocatalysts. The first step of the synthesis of Au-Pd core-shell (CS) structures involves the preparation of Au nanoparticles, employing trisodium citrate as a reducing and stabilizing agent. Then, Pd was grown onto the Au cores by reduction of H_2PdCl_4 in the presence of ascorbic acid.¹⁻² The Pd thickness was determined by the amount of Pd precursor added: the shell thicknesses were controlled to be either 1 or 10 nm, depending on the volume of H_2PdCl_4 solution added to the colloidal Au nanoparticles. The metallic nanostructures were supported on Vulcan XC-72R (Cabot).³ A set amount of the Vulcan XC-72R powder was suspended and stirred during 48 h in controlled amounts of nanoparticle dispersions, calculated to obtain a total metal loading of 20 wt %. The as-prepared carbon-supported nanoparticle powders were filtered, washed with Milli-Q water, and dried at 60 °C overnight. Samples were labelled as CS1 and CS10, when the Pd shell thicknesses aimed for were 1 and 10 nm, respectively.

Table S1 summarizes average diameters of the core-shell structures (D), shell thickness (δ) and composition of the particles obtained from at least 200 particles per sample, and their elementary composition, estimated from EDX measurements. The mass ratio from the EDX data was highly consistent with the composition of the synthesis bath, demonstrating that Pd nucleation occurs exclusively at the Au surfaces.⁴⁻⁵ The average metal loading of each sample was in the region of 15 to 19 wt %, as estimated from atomic absorption spectroscopy and energy-dispersive X-ray spectroscopy.

Structural characterization. The metal ratio was determined by energy dispersive X-ray (EDX) analysis using an Oxford Instruments ISIS 300, coupled to a JEOL JSM 5600LV scanning electron microscope. This measurement was confirmed by atomic absorption spectroscopy. A ~5 mg portion

of electrocatalysts powder was digested in aqua regia and diluted to 25 mL. The sample was analysed on a Varian SpectraAA 220, previously calibrated with known standards. Transmission electron microscopy (TEM) images were obtained using a JEOL JEM 1200 EX MKI and the image analysis software Soft Imaging Systems GmbH analySIS 3.0. High resolution TEM images in figure 1a-b were recorded with a Titan 80-300 (Fei Company). STEM-HAADF images and EDX intensity profile were obtained with a JEOL JEM 2010.

DEMS calibration. The calculation of the efficiency for formic acid conversion to CO₂ by DEMS requires a previous determination of the $m/z = 44$ calibration constant (K^{CO_2}). This constant correlates the number of CO₂ molecules generated on the electrode surface (through the faradaic charge) with the portion of this molecules captured by the mass spectrometer (proportional to $m/z = 44$ ion current). It has to be determined before each experiment because it depends of several variables (membrane-electrode gap, flow rate, temperature and pressure in the mass vacuum line). The calibration constant, K^{CO_2} is calculated as follows, where the faradaic ($Q_f^{CO_2}$) and ionic $m/z = 44$ ($Q_i^{CO_2}$) charges were calculated from CO_{ads} oxidation voltammetry, and related according to the equation:

$$K^{CO_2} = 2 \frac{Q_i^{CO_2}}{Q_f^{CO_2}} \quad (\text{eq. S1})$$

The current efficiency, \mathcal{E}^{CO_2} for formic acid electrooxidation to CO₂ is determined from the equation:

$$\mathcal{E}^{CO_2} = \frac{2 * Q_i^{CO_2}}{K^{CO_2} * Q_f^T} \quad (\text{eq. S2})$$

where Q_f^T is the total charge associated with all faradaic processes at the surface. Further details are given in previous works.⁶⁻⁷

First Principles Calculations. All calculations were performed using the DACAPO code.⁸ This utilizes an iterative scheme to solve the Kohn-Sham equations of density functional theory self-consistently. A plane-wave basis set is used to expand the electronic wave functions, and the inner electrons were represented by ultrasoft pseudopotentials,⁹ which allow the use of a low energy cut-off for the plane wave basis set. An energy cutoff 450 eV, dictated by the pseudopotential of each metal, was used. The electron-electron exchange and correlation interactions are treated with the generalized gradient approximation in the version of Perdew et *al.*¹⁰ The Brillouin-zone integration was performed using a $8 \times 8 \times 1$ k-point Monkhorst-Pack grid,¹¹ corresponding to the 1×1 surface unit cell. Spin polarization was not considered. Dipole correction was used to avoid slab-slab interactions.¹² In all the calculations a vacuum corresponding to 12 Å was used.

Table S1. Mean diameter (D), Pd thickness (δ), Au:Pd mass ratio and metal loading on the Vulcan support.

| | D / nm | δ / nm | Au:Pd mass ratio | Loading (wt %) |
|------|----------------|---------------|----------------------|----------------|
| CS1 | 21.8 ± 1.1 | 1.3 ± 0.1 | $81.3:18.7 \pm 2.4$ | 15.0 ± 1.9 |
| CS10 | 38.9 ± 1.5 | 9.9 ± 1.1 | $17.9: 82.1 \pm 0.7$ | 17.5 ± 1.4 |

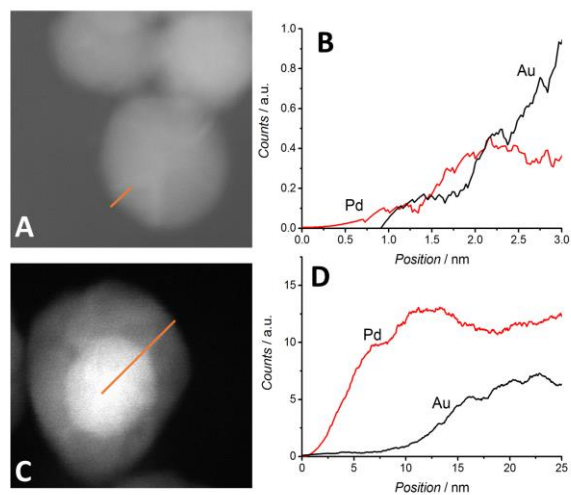


Figure S1. STEM-HAADF images and EDX intensity profile for CS1 (A, B) and CS10 (C, D) nanoparticles. The EDX profile is obtained along the orange line in the corresponding STEM image.

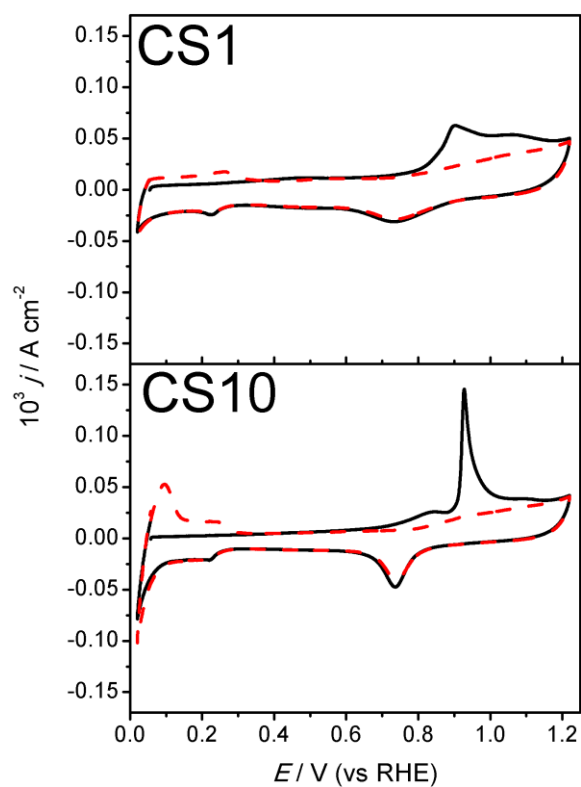


Figure S2. Cyclic voltammograms of the adsorbed CO oxidation at CS1 and CS10 catalysts in 0.5 M H_2SO_4 , recorded at 0.020 V s^{-1} . The electrode potential was held at 0.20 V vs RHE. After adsorption, and prior to recording the voltammograms, excess CO was displaced from solution by purging high purity Ar. The black full line corresponds to the first cycle, while the second cycle is displayed as a red dotted line.

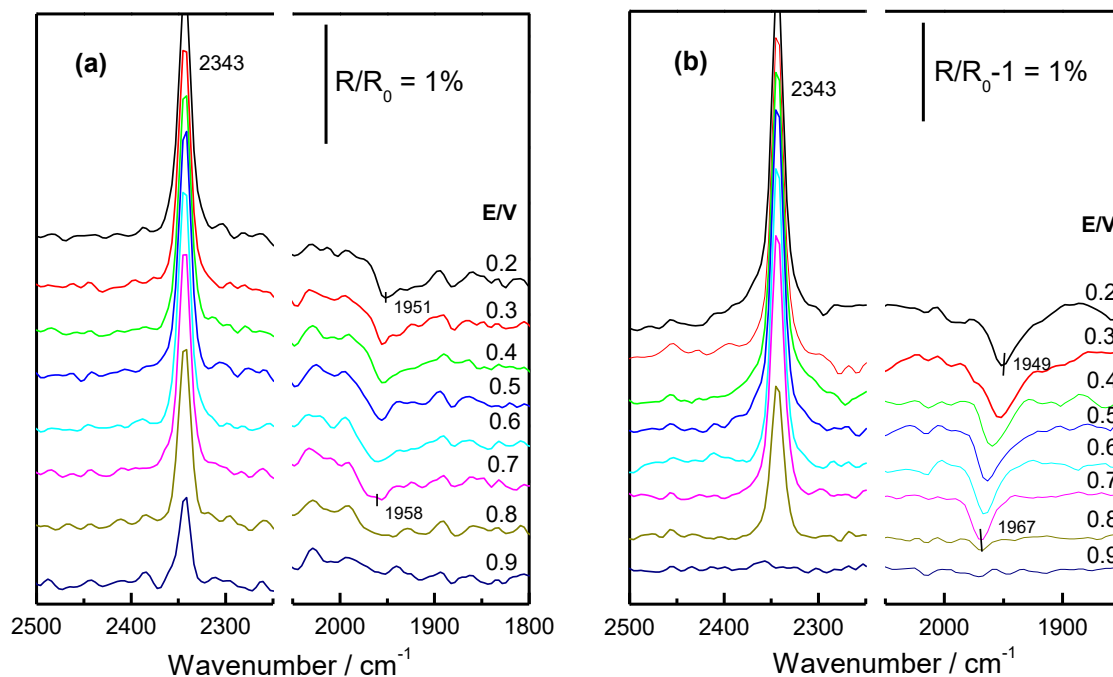


Figure S3. In situ FTIR spectra obtained during the oxidation of adsorbed CO at CS1 (a) and CS10 (b), taking the spectrum at 1.10 V as reference. Further details are given in the main paper.

REFERENCES

1. Nørskov, J. K.; Bligaard, T.; Rossmeisl, J.; Christensen, C. H., *Nat. Chem.* **2009**, *1*, 37-46.
2. Liu, P.; Nørskov, J. K., *PCCP* **2001**, *3*, 3814-3818.
3. Strasser, P.; Koh, S.; Anniyev, T.; Greeley, J.; More, K.; Yu, C.; Liu, Z.; Kaya, S.; Nordlund, D.; Ogasawara, H.; Toney, M. F.; Nilsson, A., *Nat. Chem.* **2010**, *2*, 454-460.
4. Montes de Oca, M. G.; Plana, D.; Celorrio, V.; Lazaro, M. J.; Fermín, D. J., *J. Phys. Chem. C* **2011**, *116*, 692-699.
5. Celorrio, V.; Montes de Oca, M. G.; Plana, D.; Moliner, R.; Lázaro, M. J.; Fermín, D. J., *J. Phys. Chem. C* **2012**, *116*, 6275-6282.
6. Flórez-Montaño, J.; García, G.; Guillén-Villafuerte, O.; Rodríguez, J. L.; Planes, G. A.; Pastor, E., *Electrochim. Acta* **2016**, *209*, 121-131.
7. Celorrio, V.; Calvillo, L.; Moliner, R.; Pastor, E.; Lázaro, M. J., *J. Power Sources* **2013**, *239*, 72-80.
8. Hammer, B.; Hansen, L. B.; Nørskov, J. K., *Phys. Rev. B* **1999**, *59*, 7413-7421.
9. Vanderbilt, D., *Phys. Rev. B* **1990**, *41*, 7892-7895.
10. Perdew, J. P.; Burke, K.; Ernzerhof, M., *Phys. Rev. Lett.* **1996**, *77*, 3865-3868.
11. Monkhorst, H. J.; Pack, J. D., *Phys. Rev. B* **1976**, *13*, 5188-5192.
12. Bengtsson, L., *Phys. Rev. B* **1999**, *59*, 12301-12304.